

## Article

# Hybrid Positioning Algorithm for Tilted Receiver Using RSS and TDOA with Gaussian Process

Xunhe Zuo <sup>1</sup>, Zixiong Wang <sup>1,\*</sup> , Jinlong Yu <sup>1</sup> and Yang Jiang <sup>2</sup>

<sup>1</sup> School of Electrical and Information Engineering, Tianjin University, Tianjin 300072, China; zuoxunhe@tju.edu.cn (X.Z.); yujinlong@tju.edu.cn (J.Y.)

<sup>2</sup> College of Physics, Guizhou University, Guiyang 550025, China; jiangy@gzu.edu.cn

\* Correspondence: wangzixiong@tju.edu.cn

**Abstract:** In the visible light positioning (VLP) system, the received signal strength (RSS) algorithm has a better signal noise ratio performance than the time difference of arrival (TDOA) algorithm, while the RSS algorithm needs to work under the condition that the transmitter and receiver are strictly parallel. However, the receiver is prone to tilt due to environmental disturbances, which reduces the accuracy of the RSS algorithm. For the tilted receiver, the TDOA algorithm has a higher positioning accuracy than the RSS algorithm. In order to take full advantage of the two algorithms, we propose a hybrid positioning algorithm to locate the tilted receiver by using a Gaussian process (GP). The scheme separately uses RSS and the distance difference as the inputs of the GP model to estimate the position of the receiver. Then, according to the proposed positioning selection strategy, the more credible estimated position in our opinion is selected as the final estimated position. In addition, RSS information in the hybrid algorithm is extracted from the TDOA signal, which allows the hybrid algorithm to prevent an increase in the complexity of the VLP system. During the training and testing, RSS is normalized to meet the order-of-magnitude requirements of the GP model on the input data. Simulation results validate the hybrid algorithm based on a two-dimensional positioning system for the tilted receiver. When the standard deviations of the azimuth angle and elevation angle are  $1^\circ$ , the positioning accuracy of the hybrid algorithm is 53.7% higher than that of the RSS algorithm using an artificial neural network, and 49.9% higher than that of the RSS algorithm using a GP. The localization error under  $1^\circ$  standard deviations of azimuth and elevation angles is 20.2% lower than that under  $20^\circ$  standard deviations of the two angles.



**Citation:** Zuo, X.; Wang, Z.; Yu, J.; Jiang, Y. Hybrid Positioning Algorithm for Tilted Receiver Using RSS and TDOA with Gaussian Process. *Photonics* **2023**, *10*, 538. <https://doi.org/10.3390/photronics10050538>

Received: 4 April 2023

Revised: 1 May 2023

Accepted: 4 May 2023

Published: 6 May 2023



**Copyright:** © 2023 by the authors. Licensee MDPI, Basel, Switzerland. This article is an open access article distributed under the terms and conditions of the Creative Commons Attribution (CC BY) license (<https://creativecommons.org/licenses/by/4.0/>).

**Keywords:** Gaussian process (GP); RSS; TDOA; tilted receiver; visible light positioning (VLP)

## 1. Introduction

Due to the multi-path effects, a global position system (GPS) performs poorly by attenuated satellite signals in the complicated indoor environment [1]. In order to solve this problem, the development of indoor localization technology has been put on the agenda. Indoor localization technology can be applied in many fields, including smart home robots, the express delivery industry, and personnel supervision [2]. All these applications require centimeter-level accuracy to work normally. Nowadays, mainstream indoor localization technologies include Bluetooth, WiFi, and radio frequency (RF) identification [3], which use RF signals to transmit data. However, high-frequency radio signals cause electromagnetic leakage and cause health threats to the human body [4].

With the development of the light-emitting diode (LED) industry, visible light communication (VLC) has become a new wireless communication technology to replace RF [5]. Visible light positioning (VLP) based on VLC is also considered as a new approach to indoor localization, which can act as an illumination device and provide accurate positioning services in the various application scenarios. It also prevents electromagnetic interference and information leakage due to the confined space [6]. VLP technology is generally divided into

two categories, where one is the imaging positioning method based on the features of the image captured by the sensors, and the other one is the non-imaging positioning method based on the processing of signals received by the photo-diode (PD). The non-imaging positioning method is frequently used because of low cost and simple algorithm implementation. The current mainstream non-imaging positioning methods include received signal strength (RSS), angle of arrival (AOA), time difference of arrival (TDOA), and phase difference of arrival (PDOA) [7]. These methods assume that the receiver and transmitter are parallel to each other. However, the receiver is prone to tilt due to environmental disturbances, which reduces the accuracy of the positioning algorithm [8]. Therefore, many positioning algorithms for the tilted receiver have been studied. In [9], a gyroscope is used to provide the receiver's tilted angle, and the weighting factors are introduced to compensate for the estimated position of the receiver, where the scheme achieves centimeter-level positioning accuracy. In [10], the receiver is mounted on a rotatable and retractable platform. The attitude of the receiver is constantly changed to obtain multiple sets of measurement experimental data. The position of the receiver is estimated based on the signals in different azimuths, and the positioning accuracy of algorithm is centimeter-level. Both these schemes add additional sensors to the algorithms to obtain the attitude information of the receiver, which sacrifices system cost to improve positioning accuracy.

In addition to the above positioning algorithms, machine learning (ML) algorithms have also been studied to locate the tilted receiver [11]. The ML algorithms do not describe the specific form of the physical model, but build the set of mappings between the input and output. The working mechanism prevents errors caused by inaccurate modeling and reduces the correlation with disturbances. The ML algorithms build datasets to train models in the working scenarios so as to estimate the output for a given input in the same scenario [12]. In [13], a camera is used to capture the image of LED. Then, the relationship between the features of LEDs' image and the receiver's position is established through artificial neural network (ANN) and the scheme achieves centimeter-level positioning accuracy. In [14], X-axis, Y-axis, and Z-axis coordinates of the receiver are estimated by three neural networks, respectively. The positioning accuracy of the algorithm is millimeter-scale. However, both of these schemes require large-scale training sets, which leads to an increase in time cost. Some other ML algorithms are applied to deal with this type of problem. In [15], the RSS algorithm using a Gaussian process (GP) is applied to reduce the amount of samples in the training set and the positioning accuracy is centimeter-level. For the tilted receivers, the TDOA algorithm has better positioning accuracy than the RSS algorithm, while the TDOA algorithm is sensitive to environmental interference [16]. Although the practical implementation of the TDOA algorithm is limited by various constraints, a correlated TDOA positioning system has been proposed in [17] with a final localization error of 9.2 cm. Hence, the hybrid RSS–TDOA algorithm is considered as a scheme that takes full advantage of the two algorithms.

Motivated by the above, we propose a hybrid RSS–TDOA positioning algorithm using GP to locate the tilted receiver. The contributions are summarized as follows.

- We propose a hybrid RSS–TDOA positioning algorithm for the tilted receiver. The scheme uses RSS and TDOA, respectively, in the GP model to estimate the position of the receiver. Then, according to the proposed positioning selection strategy, the more credible estimated position in the two algorithms is selected as the final estimated position of the receiver. In addition, RSS information in the hybrid algorithm is extracted from TDOA signals, which prevents the hybrid algorithm from increasing the complexity of the system compared with using two data acquisition modules to obtain different information.
- We introduce the GP algorithm to reduce the amount of samples in the training set for the ML model. Compared with other ML algorithms, the GP algorithm has better performance with a small training set. The GP model can provide us with the distribution information of the estimated target which is used in the positioning selection strategy. In addition, we derive the modified channel gain formula when

the receiver is tilted. For the case in which the tilted angle is known, the received signal strength at a certain point in space can be calculated by the modified formula, which helps us to construct the test set to evaluate the hybrid algorithm. Finally, a normalization method of GP is used to prevent accuracy degradation caused by the data imbalance.

The remainder of this article is organized as follows. Section 2 describes the principle, which includes the system model for VLP, GP, the positioning selection strategy, and normalization of GP. The hybrid RSS–TDOA positioning algorithm is proposed in Section 3. Section 4 discusses the simulation results. The conclusion is summarized in Section 5.

## 2. Principle

### 2.1. System Model

In this paper, a VLC system is considered, where four LEDs are mounted on the ceiling of the room as transmitters for illumination. The LEDs are symmetrical with respect to the center of the ceiling. The receiver is fixed on the observation plane, which receives the signals from transmitters in the VLC channel. Due to the multi-path effects, the VLC channel includes both light of sight (LOS) and non light of sight (NLOS) components [18]. We can effectively combat the multi-path effects through orthogonal frequency division multiplexing (OFDM) technology [19], so here only the LOS component needs to be considered. According to the model of Lambertian radiation, when PD’s incidence angle is smaller than PD’s field of view (FOV), the channel gain is given by [20]

$$G_{\text{LOS}} = \frac{(m + 1)A}{2\pi D^2} \cos^m(\phi) \cos(\psi) T(\psi) g(\psi), \tag{1}$$

where  $A$  is the effective area of PD, an  $D$  is the distance between the transmitter and receiver. The mode number  $m$  of Lambertian radiation is given by  $m = -\ln 2 / \ln(\cos \Phi_{1/2})$ , where  $\Phi_{1/2}$  is the semiangle at the half power of the transmitter.  $T(\psi)$  is the gain of optical filter and  $g(\psi)$  is the gain of optical concentrator.  $\phi$  and  $\psi$  are the radiation angle of the transmitter and the incident angle of the PD, respectively. When the receiver and transmitter are parallel,  $\phi$  is equal to  $\psi$ .

We consider that the transmitter is perpendicular to the ceiling and the receiver is tilted at a random altitude, as shown in Figure 1. The center of the room ground is the coordinate origin  $(0, 0, 0)$ . The coordinates of  $i$ th transmitter and receiver are  $(x_i, y_i, z_i)$  and  $(a, b, c)$ , respectively. The attitude of the receiver is described by the azimuth angle  $\alpha$  and the elevation angle  $\theta$ , where  $\alpha$  and  $\theta$  both follow the Gaussian distribution.

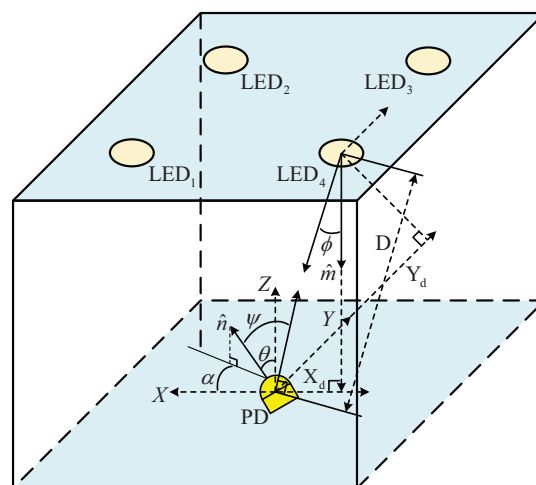


Figure 1. The system model.

The azimuth angle  $\alpha$  is the angle between the projection of the receiver’s normal vector on the X-Y plane and the X-axis. The elevation angle  $\theta$  is the angle between the Z-axis and the normal vector of the receiver. The normal vector of the receiver is defined as  $\hat{n} = [\sin(\theta) \cos(\alpha), \sin(\theta) \sin(\alpha), \cos(\theta)]^T$ . According to the law of cosines,  $\cos(\psi)$  in Equation (1) is given by

$$\cos(\psi) = \frac{X_d \sin(\theta) \cos(\alpha) + Y_d \sin(\theta) \sin(\alpha) + Z_d \cos(\theta)}{\sqrt{X_d^2 + Y_d^2 + Z_d^2}} \tag{2}$$

$X_d$  is the distance between the transmitter and receiver in the X-axis direction, which can be expressed as  $X_d = x_i - a$ .  $Y_d$  and  $Z_d$  are the distance in the Y-axis and Z-axis directions, respectively. Similarly,  $\cos(\phi)$  in Equation (1) is given by  $\cos(\phi) = Z_d / \sqrt{X_d^2 + Y_d^2 + Z_d^2}$ . Substituting Equation (2) and  $\cos(\phi)$  into Equation (1), we obtain

$$\begin{aligned} G_{\text{LOS}} &= \frac{(m+1)A}{2\pi(X_d^2 + Y_d^2 + Z_d^2)} \cos^m(\phi) \cos(\psi) T(\psi) g(\psi) \\ &= \frac{(m+1)A}{2\pi(X_d^2 + Y_d^2 + Z_d^2)} \frac{Z_d^m L_p}{(X_d^2 + Y_d^2 + Z_d^2)^{(m+1)/2}} \tag{3} \\ &= \frac{(m+1)Ah^m}{2\pi} \frac{L_p}{D^{m+3}} \end{aligned}$$

where  $L_p = X_d \sin(\theta) \cos(\alpha) + Y_d \sin(\theta) \sin(\alpha) + Z_d \cos(\theta)$ ,  $D = \sqrt{X_d^2 + Y_d^2 + Z_d^2}$ ,  $h = Z_d$  and  $T(\psi) = g(\psi) = 1$ .  $h$  is equal to the height difference between transmitter and receiver. We consider that the azimuth angle  $\alpha$  and elevation angle  $\theta$  both follow the Gaussian distribution. The probability density function (PDF) can be expressed as follows:

$$\begin{cases} f(\alpha, \mu_\alpha, \sigma_\alpha) = \frac{1}{\sqrt{2\pi}\sigma_\alpha} e^{-\frac{(\alpha - \mu_\alpha)^2}{2\sigma_\alpha^2}} \\ f(\theta, \mu_\theta, \sigma_\theta) = \frac{1}{\sqrt{2\pi}\sigma_\theta} e^{-\frac{(\theta - \mu_\theta)^2}{2\sigma_\theta^2}} \end{cases} \tag{4}$$

where  $\sigma_\alpha$  and  $\sigma_\theta$ , respectively, represent the variance in the azimuth angle and elevation angle. Additionally,  $\mu_\alpha$  and  $\mu_\theta$ , respectively, are the mean of the azimuth angle and the elevation angle. We use the localization error to evaluate the quality of the positioning algorithm, which is given by

$$E_L = \sqrt{(\hat{x} - x)^2 + (\hat{y} - y)^2} \tag{5}$$

where  $(x, y)$  are the coordinates of ground truth, and  $(\hat{x}, \hat{y})$  are the estimated coordinates of the receiver.

### 2.2. Gaussian Process

It is laborious to obtain signal information at multiple positions in the room. So, we introduce the GP algorithm to reduce the amount of samples used for the training model, which helps us to ease the workload of obtaining the dataset. GP is a supervised learning method based on non-parametric Bayesian learning and Gaussian random process [21]. In the case of small datasets, it generally performs better than other ML algorithms due to its hyperparameter tuning. Moreover, the GP model can provide the probabilistic estimation, which includes both the estimated mean and the estimated standard variance of the output for a given arbitrary input.

The GP model is defined by a mean function  $m(x)$  and a kernel function  $k(x)$ , which is expressed as  $y = f(x) \sim \text{GP}[m(x), k(x)]$  [22]. It is considered as a sampling of the multivariate Gaussian distribution, which is given by [23]

$$\begin{bmatrix} y \\ y_* \end{bmatrix} \sim N\left(0, \begin{bmatrix} K & K_*^T \\ K_* & K_{**} \end{bmatrix}\right), \tag{6}$$

where  $y$  is the output of training set consisting of known data, and  $y_*$  is the estimated output for a new input.  $K$ ,  $K_*$  and  $K_{**}$  are the kernel matrices, which are expressed as

$$\begin{aligned} K &= k(x_i, x_j) \\ K_* &= k(x_*, x_i), \\ K_{**} &= k(x_*, x_*) \end{aligned} \tag{7}$$

where  $x_i$  and  $x_j$  are two different inputs in the training set, and  $x_*$  is the new input. The parameters in kernel function are determined by exact inference, which minimizes both negative log marginal likelihood and partial derivatives of the hyperparameters. In this way, we can obtain the Gaussian distribution of estimated output  $y_*$ , which is given by [24]

$$\begin{aligned} \mu(y_*) &= K_* K^{-1} y \\ \sigma(y_*) &= K_{**} - K_* K^{-1} K_*^T \end{aligned} \tag{8}$$

The advantage of the GP model is that it can provide its statistical characteristics for each estimation, instead of requiring multiple estimations for the same input to calculate the mean and variance like other machine learning tools. The estimated output of the GP model is the linear unbiased estimate. Its mean squared error (MSE) and variance are consistent.

The GP model can be expressed as the functions  $f_1 : x_{\text{RSS}} \rightarrow \mathbb{R}^2$  and  $f_2 : x_{\text{TDOA}} \rightarrow \mathbb{R}^2$ .  $f_1$  and  $f_2$  represent the estimated coordinates of receiver. In the RSS algorithm,  $x_{\text{RSS}}$  is the received signal strength ( $x_{\text{RSS}} \in \mathbb{R}^4$ ) from different transmitters. In the TDOA algorithm,  $x_{\text{TDOA}}$  is the distance difference ( $x_{\text{TDOA}} \in \mathbb{R}^3$ ) between different transmitters. The received signal strength in the RSS algorithm can be extracted from the TDOA signal, which prevents the hybrid algorithm from increasing the complexity of the system. In order to obtain a good positioning performance, we use the data collected on the tilted receiver as the training set to train the GP model. However, it is difficult to obtain the data at different tilted angles. In the proposed algorithm, the data of the non-tilted receiver are used to train the GP model, which saves the time cost to obtain the training set. After measuring the related parameters of environmental noise and devices, the GP model can be trained by generating multiple sets of simulated values. The test set of the GP model is constructed by the channel gain formula derived in the previous section. A function that is zero everywhere is used as the mean function. The squared exponential covariance function is used as the kernel function, which is of the following form [25]

$$k(x, z) = \prod_{p=1}^D \sigma_f^2 \exp\left[-\frac{(x_p - z_p)^T P (x_p - z_p)}{2}\right], \tag{9}$$

where  $\sigma_f$  is the signal's standard variance, and  $P$  is the diagonal matrix with a characteristic length scale parameter  $D$ . There are many commonly used code packages for the GP model, including GPML, GPstuff, GPflow, and GPyTorch. Among them, GPML is known for its simple calling method and clear code logic, which is used as the implementation tool for the proposed hybrid algorithm using GP.

### 2.3. The Positioning Selection Strategy

After obtaining the estimated positions of the two algorithms, we need to decide which one is more credible. When the receiver is tilted, the localization error of the TDOA

algorithm is smaller than that of the RSS algorithm. However, the TDOA algorithm is more susceptible to environmental interference, which leads to unstable localization. In order to improve the positioning accuracy, we apply a selection strategy based on the estimated positions of the two algorithms. The GP model can provide the mean and standard deviation of the estimated positions, which can be used for the following inferences. When the mean of estimated position based on the TDOA algorithm is close to that based on the RSS algorithm, and the standard variance of estimated position based on TDOA algorithm is large, it can be considered that the estimated position of the RSS algorithm is more credible at this time. Otherwise, the estimated position of the TDOA algorithm is considered to be more credible. The selection strategies are expressed as

$$P_{\text{final}} = \begin{cases} P_{\text{RSS}} & \frac{|P_{\text{RSS}} - P_{\text{TDOA}}|}{\sigma_{\text{TDOA}}} \leq P_{\text{th}} \\ P_{\text{TDOA}} & \text{otherwise.} \end{cases}, \tag{10}$$

where  $P_{\text{RSS}}$  is the mean of the estimated position based on the RSS algorithm,  $P_{\text{TDOA}}$  is the mean of the estimated position based on the TDOA algorithm,  $|\cdot|$  is the Euclidean distance between two points in space,  $\sigma_{\text{TDOA}}$  is the standard deviation of the position estimated by the TDOA algorithm, and  $P_{\text{th}}$  is the decision threshold and its optimal value can be obtained by multiple tests.

#### 2.4. Normalization of Gaussian Process

In the above calculation, we need to be careful about the data imbalance problem. It refers to the phenomenon that in ML algorithms, if there is an excessive order of magnitude difference between the input and output of the model, it leads to performance degradation. The output of the GP model is the estimated coordinate of the receiver, whose magnitude depends on the size of the room. The input of the GP model in the TDOA algorithm is the distance differences, whose magnitude is close to that of this model's output. However, in the RSS algorithm, the magnitude of the received signal strength ranges from  $10^{-12}$  to  $10^{-6}$ , which leads to the data imbalance. Therefore, the received signal strength needs to be normalized, which is expressed as

$$R' = \frac{R - \frac{1}{N} \sum_{i=1}^N R_i}{R}. \tag{11}$$

$R'$  is the normalized received signal strength that is used for calculation in the GP model.  $R_i$  is an item in the received strength dataset, which contains the received signal strength of the non-tilted receiver from different transmitters.  $N$  is the length of the dataset.  $R$  can either be a set of known inputs in the received signal strength dataset during the training of the GP model or a new set of inputs during the evaluation of the performance of the GP model.

### 3. Hybrid RSS–TDOA Positioning Algorithm

Based on the content mentioned above, we propose a hybrid RSS–TDOA positioning algorithm for the tilted receiver. Figure 2 depicts the schematic diagram of the hybrid algorithm. In the offline stage, considerable amounts of RSS and TDOA information are measured in the room as the training set. Then, we calculate the mean of the measured RSS information and normalize all the RSS information according to the proposed normalization method. The RSS and TDOA information are used to train the GP model, respectively, and thus the offline process ends. In the online stage, the real-time measured RSS and TDOA information is, respectively, input to the GP model for estimation, and the more reliable one of the two estimations output by the GP model is determined by the proposed positioning selection strategy, which is considered as the final estimated position.

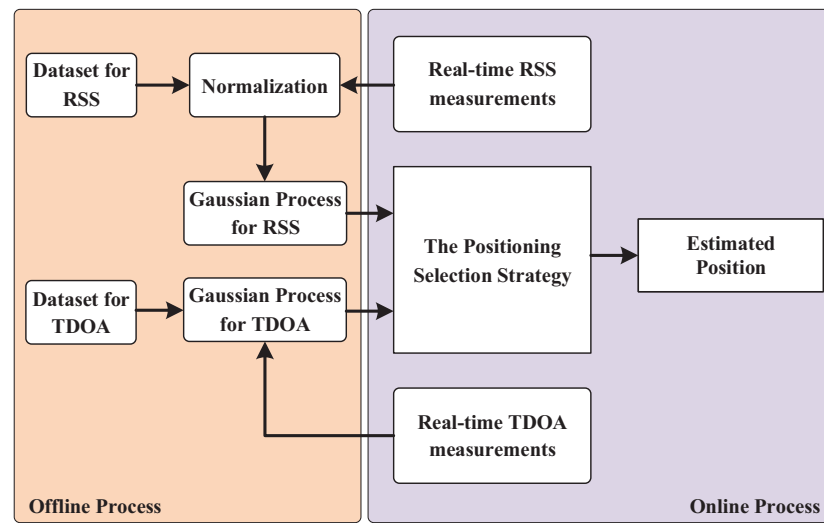


Figure 2. Schematic diagram of the hybrid positioning algorithm based on GP.

### 4. Simulation

#### 4.1. Simulation Setup

We consider an indoor VLP system, where the room size is 8 m × 8 m × 6 m. The LEDs are mounted on the ceiling and their coordinates are (2, 2, 6), (2, -2, 6), (-2, 2, 6), and (-2, -2, 6), which are driven by multiple quadrature amplitude modulation (MQAM) with OFDM signals. The receiver is placed randomly in the room at a height of 0.8 m above the floor, which has sufficient FOV to receive signals from any transmitter. The receiver uses passive PD to capture optical signals, which saves energy compared with active positioning systems such as an image sensor [26]. Table 1 depicts the specific parameters of the transmitter and receiver, including the tilted angle, the number of LED, the LEDs’ power, etc. The power of the OFDM signal is identical for each LED. To simplify the scheme, we assume that no obstacles between the transmitter and receiver can be found in the room. The localization error when cumulative density functions (CDFs) are 95% is used as the standard to evaluate the performance of the algorithm under different conditions, which is denoted as the P95-error.

Table 1. The system parameters of the simulation setup.

Parameters	Values
Number of LEDs	4
Height of receiver	0.8 m
Power of OFDM signal for each LED	3.75 W
Size of training set for GP model	100
Size of test set for GP model	101 × 101
Standard deviation of the tilted receiver	$\sigma_\alpha = \sigma_\theta = 1^\circ$
Standard deviation of the distance difference error in TDOA algorithm	$\sigma_d = 1$ cm
The semiangle at half power	60°
The Lambertian radiation pattern	1
The responsivity of PD	0.6 A/W
Bandwidth	100 MHz

#### 4.2. Simulation Results and Discussions

##### 4.2.1. Effect of Training Set Size on Positioning Performance

Firstly, we investigate the effect of training set size on the performance of the hybrid positioning algorithm. The standard deviations of the azimuth angle  $\sigma_\alpha$  and elevation angle  $\sigma_\theta$  are set to 1°. The training set size  $N$  is taken as 64, 100, 144, and 196, respectively. Figure 3 depicts the CDFs of localization error for various training set sizes. P95-error for

$N = 196$  is 4.58 cm, P95-error for  $N = 144$  is 4.75 cm, P95-error for  $N = 100$  is 4.98 cm, and P95-error for  $N = 64$  is 6.96 cm. As the training set size  $N$  increases, the localization error of the hybrid algorithm decreases. When  $N$  is equal to 100, 144, or 196, the localization error is approximately the same. The large training set increases the time cost. Therefore, we can ease the workload by selecting a reliable training set size. When the training set size  $N$  is increased to 1024, the positioning accuracy is not remarkably improved, because the training set of the GP model is too large to cause an overfitting problem. So, we chose 100 as the size  $N$  of the training set according to the simulation results.

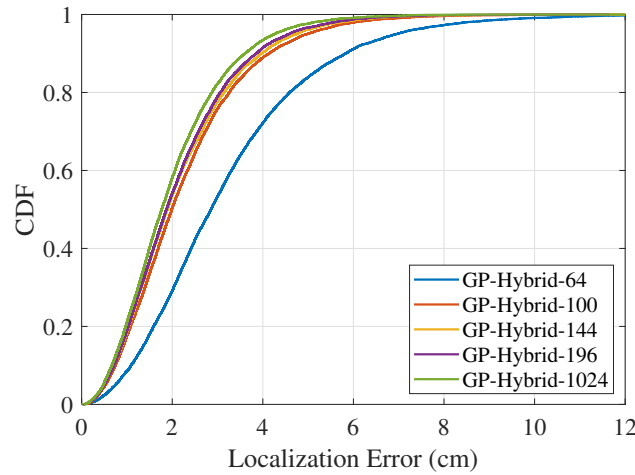


**Figure 3.** The CDFs of the localization error when  $\sigma_\alpha = \sigma_\theta = 1^\circ, \sigma_d = 1 \text{ cm}, P_{th} = 0.3$  for various sizes  $N$  of training sets.

#### 4.2.2. Effect of Decision Threshold on Positioning Performance

Secondly, we study the relationship between positioning accuracy and decision threshold  $P_{th}$ . When the training set size  $N$  is 100, the standard deviations of the azimuth angle  $\sigma_\alpha$  and elevation angle  $\sigma_\theta$  are both  $1^\circ$ . Figure 4 depicts the CDFs of localization error for various values of  $P_{th}$ . The positioning accuracy decreases with the increase in decision threshold  $P_{th}$ . When  $P_{th}$  is greater than 0.9, the P95-error is at least 6.25 cm. The P95-error drops to 4.98 cm when  $P_{th}$  decreases to 0.3. This is because the trust of the TDOA algorithm increases as  $P_{th}$  decreases. The positioning accuracy of the TDOA algorithm is higher than that of the RSS algorithm in this scenario. Therefore, we set the decision threshold  $P_{th}$  to 0.3 for high positioning accuracy.

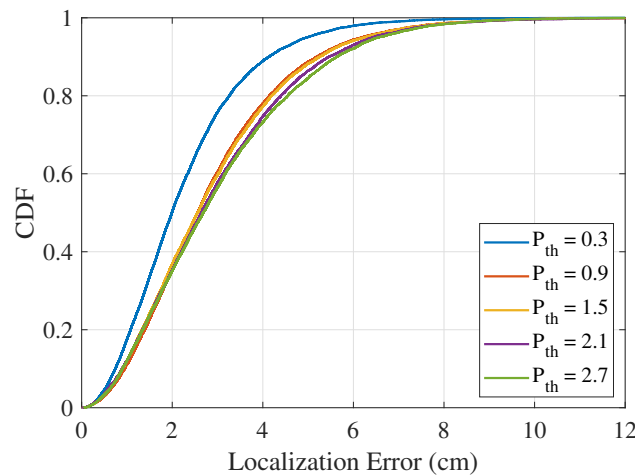


**Figure 4.** The CDFs of the localization error when  $\sigma_\alpha = \sigma_\theta = 1^\circ, \sigma_d = 1 \text{ cm}, N = 100$  for various decision thresholds  $P_{th}$ .

#### 4.2.3. Effect of Standard Variance of Receiver’s Tilted Angle on Positioning Performance

Thirdly, we investigate the effect of standard variance of the receiver’s tilted angle on the positioning accuracy. We assume that both  $\sigma_\alpha$  and  $\sigma_\theta$  are equal to  $\sigma$ . Figure 5 depicts the CDFs of localization error for various values of  $\sigma$ . The P95-error for  $\sigma = 1^\circ$  is 4.98 cm. As the standard variance  $\sigma$  increases, the P95-error for  $\sigma = 20^\circ$  increases to 6.24 cm. When the standard variance of the tilted angle increases, the P95-error increases slowly, which shows that the hybrid algorithm adapts to the changing environment well.

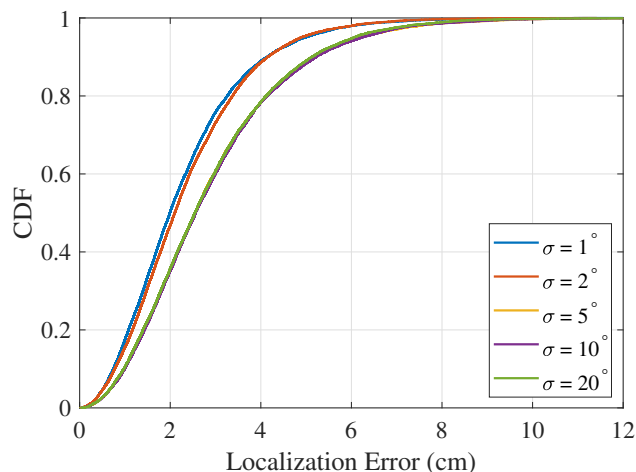


**Figure 5.** The CDFs of the localization error when  $N = 100$ ,  $\sigma_d = 1$  cm,  $P_{th} = 0.3$  for various  $\sigma_\alpha$  and  $\sigma_\theta$  ( $\sigma = \sigma_\alpha = \sigma_\theta$ ).

#### 4.2.4. Positioning Performance Comparison of Different ML Algorithms and Hybrid Algorithm

Fourthly, we compare the positioning accuracy of the hybrid algorithm with other ML algorithms including ANN-RSS, GP-RSS. The hidden layer of ANN for comparison has two layers where the numbers of neurons are 6 and 3, respectively. Figure 6 depicts the CDFs of localization error for various algorithms. P95-error for the GP-Hybrid is 4.98 cm, P95-error for GP-RSS is 9.94 cm, and P95-error for ANN-RSS is 10.75 cm. The positioning accuracy of the positioning algorithm using GP is higher than when using ANN. It is consistent with the expectation that the GP algorithm is better than the ANN algorithm with the small training set. The proposed hybrid positioning algorithm is more suitable for the situation of the tilted receiver than that based on the RSS. This is because when the accuracy of the RSS algorithm is affected by the tilted angle of the receiver, the TDOA algorithm has an advantage in the positioning selection strategy so that an objective final positioning result can still be obtained. Additionally, if TDOA information is delayed for some reason, the hybrid algorithm can still locate the receiver through RSS information. The robustness of the VLP system refers to the ability of the receiver to provide relatively accurate positioning results when the quality of measurement data degrades [27]. Regarding the proposed hybrid algorithm, if either the TDOA or RSS algorithm is not interrupted, the accuracy of the hybrid algorithm can be achieved, which guarantees the robustness.

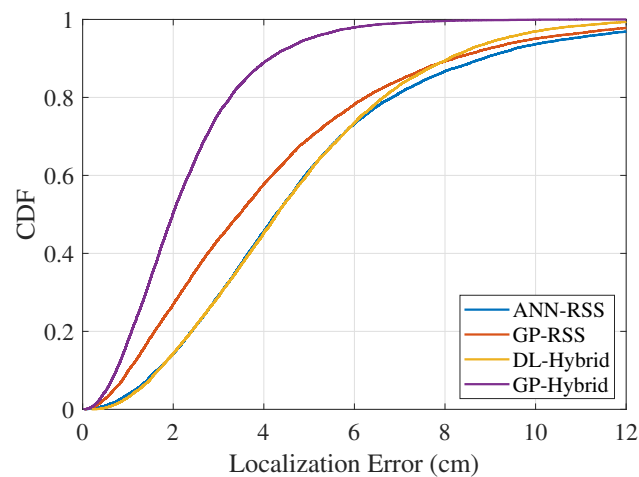


**Figure 6.** The CDFs of the localization error when  $N = 100$ ,  $\sigma_\alpha = \sigma_\theta = 1^\circ$ ,  $\sigma_d = 1$  cm,  $P_{th} = 0.3$  for various ML algorithms.

In Figure 6, we also compare a deep learning (DL)-hybrid algorithm with the proposed hybrid algorithm to show the superiority of the GP algorithm. The DL network used for comparison is transformed from the VGGish network model, and it uses the Adam optimizer in the training. The maximum number of epochs and minimum batch size used for training are set to 400 and 64, respectively. The initial learning rate and gradient threshold are set to 0.002 and 1, respectively. The number of the training set is set to 196 to observe the performance of the deep learning network under the largest training set. The input of the DL network is the combined information of the RSS and TDOA, and the output is the estimation of the receiver's three-dimensional coordinates. The performance of the DL algorithm is slightly better than that of the ANN algorithm, indicating that the multi-layer network has a better positioning accuracy for the tilted receiver. However, even with a considerable number of training sets, the performance of the DL network still lags behind the GP algorithm when the training set size  $N$  is 100, which shows that the GP algorithm is more suitable for working with small-scale training sets than the DL network.

#### 4.2.5. Positioning Performance and Prospect of Hybrid Algorithm in Three-Dimensional (3D) Positioning System

Lastly, we investigate the performance of the proposed algorithm in a three-dimensional (3D) positioning system. The training set of the GP model is still the received data of the non-tilted receiver installed at a height of 0.8 m. The height of receivers in the test set is changed to a normal distribution with a mean of 0.8 m and a standard deviation of 0.05 m. Due to the addition of the one-dimensional estimation coordinate, the training set sizes of the GP model are increased to at least 144. Figure 7 depicts the CDFs of localization error in the 3D positioning system for various training set sizes. The P95-errors for  $N = 144, 196, 324, 400$  are all about 11.55 cm. As the size of the training set increases, we can build the datasets at multiple heights to train the GP model, which obtains better positioning performance compared to acquiring the datasets at a fixed height.

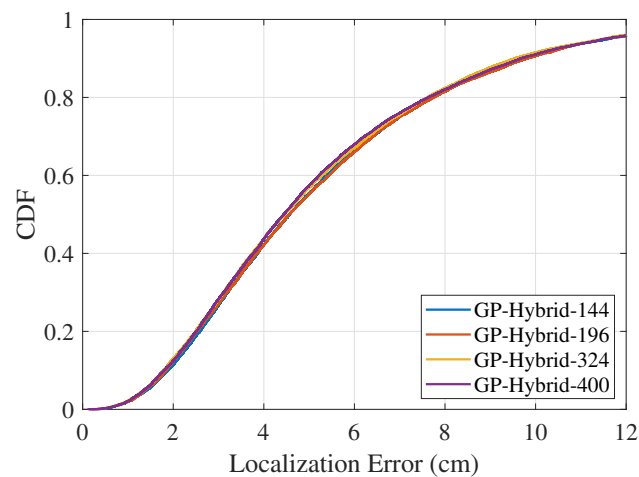


**Figure 7.** The CDFs of the localization error in a 3D positioning system when  $\sigma_\alpha = \sigma_\theta = 1^\circ$ ,  $\sigma_d = 1$  cm,  $P_{th} = 0.3$  for various sizes  $N$  of training sets.

## 5. Conclusions

This paper proposes a hybrid RSS–TDOA positioning algorithm using GP for the case of the tilted receiver. The scheme uses, separately, RSS and distance difference as the inputs of the GP model to estimate the position of the receiver. According to the proposed positioning selection strategy, the more credible one in the estimated positions of the two algorithms is selected as the final estimated position. In addition, the scheme eases the workload of obtaining the training set by introducing the GP algorithm. In the simulation, we study the effects of training set size and decision threshold on the performance of the hybrid algorithm. We also compare the performance of different ML algorithms and investigate the performance of the hybrid algorithm at different standard variances of the tilted angle. The simulation results show that the performance of the positioning algorithm using GP is better than that using ANN with the small training set. By adjusting the parameters including the size of the training set and the decision threshold, the hybrid algorithm still performs well when the receiver is tilted seriously. When the standard deviations  $\sigma_\alpha$  and  $\sigma_\theta$  of the tilted angle are  $1^\circ$ , the positioning accuracy of the hybrid algorithm is 53.7% higher than that of the ANN–RSS algorithm, and 49.9% higher than that of the GP–RSS algorithm.

**Author Contributions:** Conceptualization, X.Z. and Z.W.; software, X.Z.; validation, X.Z., Z.W., J.Y. and Y.J.; writing—original draft preparation, X.Z.; writing—review and editing, Z.W., J.Y. and Y.J.; supervision, Z.W., J.Y. and Y.J. All authors have read and agreed to the published version of the manuscript.

**Funding:** This research was supported by the National Natural Science Foundation of China under Grant 61835003 and Grant 62005194.

**Institutional Review Board Statement:** Not applicable.

**Informed Consent Statement:** Not applicable.

**Data Availability Statement:** Not applicable.

**Conflicts of Interest:** The authors declare no conflict of interest.

## References

1. Liu, H.; Darabi, H.; Banerjee, P.; Liu, J. Survey of Wireless Indoor Positioning Techniques and Systems. *IEEE Trans. Syst. Man Cybern. Part C Appl. Rev.* **2007**, *37*, 1067–1080. [[CrossRef](#)]
2. Hua, L.; Zhuang, Y.; Li, Y.; Wang, Q.; Zhou, B.; Qi, L.; Yang, J.; Cao, Y.; Haas, H. FusionVLP: The Fusion of Photodiode and Camera for Visible Light Positioning. *IEEE Trans. Veh. Technol.* **2021**, *70*, 11796–11811. [[CrossRef](#)]
3. Zafari, F.; Gkelias, A.; Leung, K.K. A Survey of Indoor Localization Systems and Technologies. *IEEE Commun. Surv. Tutor.* **2019**, *21*, 2568–2599. [[CrossRef](#)]

4. Valberg, P.A.; Van Deventer, T.E.; Repacholi, M.H. Workgroup Report: Base Stations and Wireless Networks—Radiofrequency (RF) Exposures and Health Consequences. *Environ. Health Perspect.* **2007**, *115*, 416–424. [[CrossRef](#)] [[PubMed](#)]
5. Wu, S.; Wang, H.; Youn, C.H. Visible Light Communications for 5G Wireless Networking Systems: From Fixed to Mobile Communications. *IEEE Netw.* **2014**, *28*, 41–45. [[CrossRef](#)]
6. Cheema, A.; Alsmadi, M.; Ikki, S. Distance Estimation in Visible Light Communications: The Case of Imperfect Synchronization and Signal-Dependent Noise. *IEEE Trans. Veh. Technol.* **2021**, *70*, 11044–11049. [[CrossRef](#)]
7. Zhou, B.; Lau, V.; Chen, Q.; Cao, Y. Simultaneous Positioning and Orientating for Visible Light Communications: Algorithm Design and Performance Analysis. *IEEE Trans. Veh. Technol.* **2018**, *67*, 11790–11804. [[CrossRef](#)]
8. Xu, H.; An, F.; Wen, S.; Yan, Z.; Guan, W. Three-Dimensional Indoor Visible Light Positioning with a Tilt Receiver and a High Efficient LED-ID. *Electronics* **2021**, *10*, 1265. [[CrossRef](#)]
9. Jeong, E.M.; Yang, S.H.; Kim, H.S.; Han, S.K. Tilted receiver angle error compensated indoor positioning system based on visible light communication. *Electron. Lett.* **2013**, *49*, 890–892. [[CrossRef](#)]
10. Li, Q.; Wang, J.; Huang, T.; Wang, Y. Three-dimensional indoor visible light positioning system with a single transmitter and a single tilted receiver. *Opt. Eng.* **2016**, *55*, 103–106. [[CrossRef](#)]
11. Huy Q, T.; Cheolkeun, H. Machine learning in indoor visible light positioning systems: A review. *Neurocomputing* **2022**, *491*, 117–131.
12. Chaudhary, N.; Alves, L.N.; Ghassembley, Z. Current Trends on Visible Light Positioning Techniques. In Proceedings of the 2019 2nd West Asian Colloquium on Optical Wireless Communications (WACOWC), Tehran, Iran, 27–28 April 2019; pp. 100–105.
13. Yuan, T.; Xu, Y.; Wang, Y.; Han, P.; Chen, J. A Tilt Receiver Correction Method for Visible Light Positioning Using Machine Learning Method. *IEEE Photonics J.* **2018**, *10*, 7909312. [[CrossRef](#)]
14. Alonso-González, I.; Sánchez-Rodríguez, D.; Ley-Bosch, C.; Quintana-Suárez, M.A. Discrete Indoor Three-Dimensional Localization System Based on Neural Networks Using Visible Light Communication. *Sensors* **2018**, *18*, 1040. [[CrossRef](#)] [[PubMed](#)]
15. Knudde, N.; Raes, W.; De Bruycker, J.; Dhaene, T.; Stevens, N. Data-Efficient Gaussian Process Regression for Accurate Visible Light Positioning. *IEEE Commun. Lett.* **2020**, *24*, 1705–1709. [[CrossRef](#)]
16. Zhang, S.; Du, P.; Chen, C.; Zhong, W.D.; Alphones, A. Robust 3D Indoor VLP System Based on ANN Using Hybrid RSS/PDOA. *IEEE Access* **2019**, *7*, 47769–47780. [[CrossRef](#)]
17. Du, P.; Zhang, S.; Chen, C.; Alphones, A.; Zhong, W.D. Demonstration of a Low-Complexity Indoor Visible Light Positioning System Using an Enhanced TDOA Scheme. *IEEE Photonics J.* **2018**, *10*, 1–10. [[CrossRef](#)]
18. Feng, L.; Yang, H.; Hu, R.Q.; Wang, J. MmWave and VLC-Based Indoor Channel Models in 5G Wireless Networks. *IEEE Wirel. Commun.* **2018**, *25*, 70–77. [[CrossRef](#)]
19. Wu, S.; Bar-Ness, Y. OFDM Systems in the Presence of Phase Noise: Consequences and Solutions. *IEEE Trans. Commun.* **2004**, *52*, 1988–1996. [[CrossRef](#)]
20. Zeng, L.; O'Brien, D.C.; Minh, H.L.; Faulkner, G.E.; Lee, K.; Jung, D.; Oh, Y.; Won, E.T. High Data Rate Multiple Input Multiple Output (MIMO) Optical Wireless Communications Using White LED Lighting. *IEEE J. Sel. Areas Commun.* **2009**, *27*, 1654–1662. [[CrossRef](#)]
21. Liu, H.; Ong, Y.S.; Shen, X.; Cai, J. When Gaussian Process Meets Big Data: A Review of Scalable GPs. *IEEE Trans. Neural Netw. Learn. Syst.* **2020**, *31*, 4405–4423. [[CrossRef](#)]
22. Williams, C.K.; Rasmussen, C.E. *Gaussian Processes for Machine Learning*; MIT Press: Cambridge, MA, USA, 2006; Volume 2.
23. Liu, K.; Hu, X.; Wei, Z.; Li, Y.; Jiang, Y. Modified Gaussian Process Regression Models for Cyclic Capacity Prediction of Lithium-Ion Batteries. *IEEE Trans. Transp. Electrification* **2019**, *5*, 1225–1236. [[CrossRef](#)]
24. Williams, C.; Barber, D. Bayesian Classification With Gaussian Processes. *IEEE Trans. Pattern Anal. Mach. Intell.* **1998**, *20*, 1342–1351. [[CrossRef](#)]
25. Duvenaud, D.K.; Nickisch, H.; Rasmussen, C. Additive Gaussian Processes. In *NIPS'15: Proceedings of the 28th International Conference on Neural Information Processing Systems*; Shawe-Taylor, J., Zemel, R., Bartlett, P., Pereira, F., Weinberger, K., Eds.; MIT Press: Cambridge, MA, USA, 2011; Volume 24.
26. Singh, J.; Raza, U. Passive Visible Light Positioning Systems: An Overview. In *Proceedings of the Workshop on Light Up the IoT*; ACM: New York, NY, USA, 2020; pp. 48–53.
27. Carreño, C.; Krommenacker, N.; Charpentier, P. Resilience and Robustness in Visible Light Positioning Systems: An introductory Approach. *IFAC-PapersOnLine* **2022**, *55*, 95–100. [[CrossRef](#)]

**Disclaimer/Publisher's Note:** The statements, opinions and data contained in all publications are solely those of the individual author(s) and contributor(s) and not of MDPI and/or the editor(s). MDPI and/or the editor(s) disclaim responsibility for any injury to people or property resulting from any ideas, methods, instructions or products referred to in the content.